JACS
JOURNAL OF THE AMERICAN CHEMICAL SOCIETY

COMMUNICATION

pubs.acs.org/JACS

Controlled Synthesis and Size-Dependent Polarization Domain Structure of Colloidal Germanium Telluride Nanocrystals

Mark J. Polking,[†] Haimei Zheng,[‡,§] Ramamoorthy Ramesh,[*,†,∥] and A. Paul Alivisatos[*,‡,∥]

[†]Department of Materials Science and Engineering and [‡]Department of Chemistry, University of California, Berkeley, California 94720, United States

[§]National Center for Electron Microscopy and [∥]Materials Sciences Division, Lawrence Berkeley National Laboratory, Berkeley, California 94720, United States

Supporting Information

ABSTRACT: Germanium telluride (GeTe) exhibits interesting materials properties, including a reversible amorphous-to-crystalline phase transition and a room-temperature ferroelectric distortion, and has demonstrated potential for nonvolatile memory applications. Here, a colloidal approach to the synthesis of GeTe nanocrystals over a wide range of sizes is demonstrated. These nanocrystals have size distributions of 10−20% and exist in the rhombohedral structure characteristic of the low-temperature polar phase. The production of nanocrystals of widely varying sizes is facilitated by the use of Ge(II) precursors with different reactivities. A transition from a monodomain state to a state with multiple polarization domains is observed with increasing size, leading to the formation of richly faceted nanostructures. These results provide a starting point for deeper investigation into the size-scaling and fundamental nature of polar-ordering and phase-change processes in nanoscale systems.

Semiconducting IV−VI nanocrystals have received attention recently due to their strong quantum size effects[1−3] and rich array of phase transitions that influence their electronic, optical, and phononic properties.[4,5] The semiconductor germanium telluride (GeTe) in particular has garnered interest due to its reversible amorphous-to-crystalline phase transition[6,7] and ferroelectric phase transition, which leads to a spontaneous polarization along a ⟨111⟩ axis below ∼625 K.[8−10] This polar distortion also leads to the formation of polarization domain boundaries, which influence its mechanical, electronic, thermal, and other properties.[11] The simplest possible ferroelectric, GeTe provides a simple model system for the study of polar-ordering phenomena at reduced dimensions, including the question of a critical length scale for the emergence of a polarization domain structure. Although the high bulk carrier density of GeTe hinders direct measurement of the spontaneous polarization, the interplay of structural, optical, electronic, and other properties makes this an important system for further study.

Despite interest in GeTe, methods for the synthesis of high-quality nanomaterials of GeTe are relatively unexplored, and little is currently known about its nanoscale properties. While vapor-phase syntheses of GeTe nanowires and solution-phase syntheses of micrometer-scale crystals and amorphous nanoparticles have been reported,[12−16] the size scales of these materials are far from the quantum regime, and the formation of crystalline GeTe of controlled sizes has remained elusive. In addition, while colloidal chemistry has proven highly successful for the synthesis of semiconducting and metallic nanomaterials with tunable optical, magnetic, and other functionalities, few syntheses of low-dimensional nanostructures of materials exhibiting spontaneous polar ordering exist,[17−19] hindering fundamental study of polar phenomena at nanoscale dimensions. Here, we describe a simple and highly adaptable synthesis of GeTe nanocrystals of sizes ranging from 8 to 100 nm using colloidal chemistry. These nanocrystals have narrow size distributions and exhibit the rhombohedral structure characteristic of the polar phase down to particle sizes of less than 10 nm. We observe a transition from a primarily monodomain state to a multidomain state for length scales above ∼30 nm, indicating a critical size scale for the emergence of a polarization domain structure.

GeTe nanocrystals with average sizes of 8, 17, and 100 nm were synthesized by reaction of the divalent germanium precursors Ge(II) chloride−1,4 dioxane complex and bis[bis(trimethylsilyl)amino]Ge(II) ($(TMS_2N)_2Ge$) with trioctylphosphine-tellurium (TOP-Te). Phase-pure GeTe nanocrystals can be prepared in a variety of solvents, including 1,2-dichlorobenzene, 1-octadecene, phenyl ether, and others. The basic chemistry is also compatible with other surfactants, including 1-dodecanethiol, oleylamine, and phosphonic acids.

Nanocrystals with an average diameter of 8 nm were synthesized by the reaction of $(TMS_2N)_2Ge$ with TOP-Te in the presence of 1-dodecanethiol and excess trioctylphosphine at 230 °C, and nanocrystals with a 17 nm average diameter were prepared using the same precursors in the presence of oleylamine at 250 °C. The synthesis of nanocrystals with an average size of 100 nm was accomplished through the use of $GeCl_2$−dioxane complex and TOP-Te in the presence of 1-dodecanethiol at 180 °C. Prior to the syntheses, solvents were dried and degassed where appropriate, which was found to be crucial to the production of phase-pure GeTe. Full details on all syntheses are provided in the Supporting Information (SI).

The production of GeTe nanocrystals in two size regimes is facilitated by the use of two precursors, $GeCl_2$−dioxane complex and $(TMS_2N)_2Ge$, with vastly different reaction kinetics. The

Received: September 14, 2010
Published: January 31, 2011

dx.doi.org/10.1021/ja108309s | J. Am. Chem. Soc. 2011, 133, 2044–2047

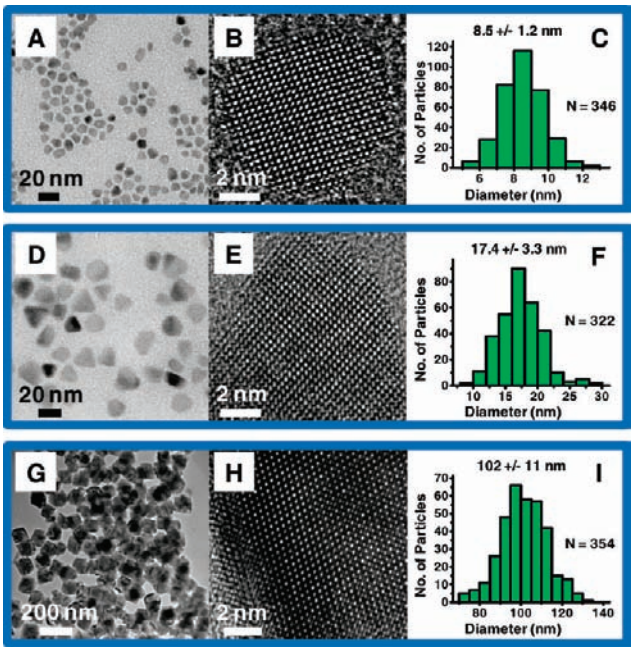

Figure 1. Transmission electron microscope (TEM) images and size statistics for GeTe nanocrystals. (A−C) Low-resolution TEM image (A), high-resolution TEM (HRTEM) image (B), and size statistics (C) for 8 nm GeTe nanocrystals. (D−F) Low-resolution TEM image (D), HRTEM image (E), and size statistics (F) for 17 nm GeTe nanocrystals. (G−I) Low-resolution TEM image (G), HRTEM image (H), and size statistics (I) for 100 nm GeTe nanocrystals. *N* is the number of particles measured.

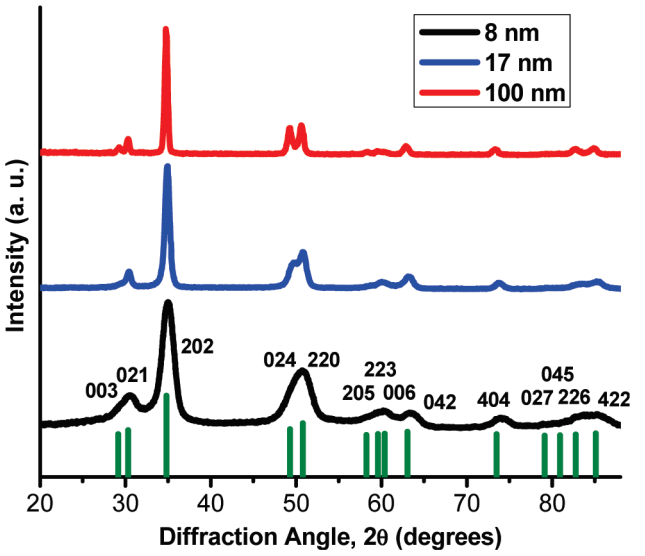

Figure 2. Powder X-ray diffraction patterns for 8, 17, and 100 nm GeTe nanocrystals. The patterns indicate the presence of phase-pure GeTe in the rhombohedral *R*3*m* (160) space group.

latter precursor often yielded nucleation within several seconds in many different surfactant/solvent systems, whereas the former reacted sluggishly, if at all, under the same reaction conditions. Both precursors are readily reduced in the presence of primary amines and alkanethiols to yield Ge(0) nanocrystals. $GeCl_2$−dioxane reacts sluggishly with pure oleylamine at 300 °C and produces germanium nanocrystals with an average size of approximately 15 nm (SI, Figure S1A); reduction of $(TMS_2N)_2Ge$ under the same reaction conditions results in rapid nucleation of ∼3 nm particles (Figure S1B). Similar trends are observed at lower temperatures. Although the precise reaction mechanism is not fully understood, this large increase in the Ge(II) reduction rate may contribute to the increase in particle nucleation rate and decrease in diameter from $GeCl_2$−dioxane to $(TMS_2N)_2Ge$, consistent with a previous study indicating the vital role of Ge(II) reduction kinetics in GeTe formation.[15]

Typical transmission electron microscope (TEM) images for 8, 17, and 100 nm nanocrystals are shown in Figure 1. High-resolution TEM (HRTEM) imaging indicates that particles of all sizes are crystalline, and size statistics collected on samples of over 250 particles demonstrate size distributions of 10−20%, typical values for many colloidal syntheses.

Powder X-ray diffraction (XRD, Figure 2) was performed with a Bruker AXS GADDS D-8 diffractometer (Co Kα, 1.79026 Å). All patterns confirm the presence of phase-pure GeTe. The polar phase transition in GeTe from a rock salt structure to a rhombohedral structure results in the splitting of the 111 and 220 diffraction lines (in the cubic indexing system) into 003−021 and 024−220 doublets (in the rhombohedral indexing system).[9,10] The XRD patterns of the 17 and 100 nm particles exhibit clear splitting of the 111 and 220 doublets characteristic of the rhombohedral phase. Significant peak broadening for the 8 nm particles, however, complicates determination of the material phase, necessitating analysis by Rietveld refinement (SI, Figure S2). This analysis confirms the presence of the rhombohedral phase with a rhombohedral angle of approximately 88.5°. Multiple trials consistently indicated a rhombohedral distortion.

TEM and electron diffraction studies (Figures 3 and 4) reveal the size-dependent evolution from a primarily monodomain state to a state with multiple polarization domains. Many IV−VI materials form in low-symmetry structures with weak bonding along certain crystallographic directions, leading to stacking faults, twin boundaries, and other defects.[4,20] GeTe in the rhombohedral phase forms {100} and {110} twin boundaries as well as inversion boundaries separating domains with different ⟨111⟩ polarization axes.[11] HRTEM investigations of the 8 and 17 nm particles indicate that these particles primarily consist of a single domain. Electron diffraction patterns of the 100 nm particles, in contrast, reveal splitting of diffraction spots consistent with the formation of {100} and {110} twin boundaries (Figure 3), and scanning electron microscope (SEM) and Z-contrast TEM imaging (SI, Figure S3) show extensive faceting. The change in lattice orientation across {100} and {110} domain boundaries leads to pronounced diffraction contrast in dark-field images.[21] The breakdown of Friedel symmetry for noncentrosymmetric crystals leads to differences in background contrast between inversion domains in dark-field images, and observation using complementary $\vec{g}$ and $-\vec{g}$ diffraction vectors results in a reversal of the relative contrast.[21] Dark-field TEM images of the 100 nm particles (Figure 3) reveal the presence of all three types of domain boundaries and the spatial relationships between domains. These images suggest that the 100 nm particles are largely bidomain. The electron diffraction patterns of the 8 nm particles (SI, Figure S4), in contrast, contain a single set of spots, and dark-field TEM images reveal largely uniform contrast, confirming the monodomain structure.

To study the domain structure in still larger particles, additional precursor was injected into a solution containing seed

dx.doi.org/10.1021/ja108309s |*J. Am. Chem. Soc.* 2011, 133, 2044–2047

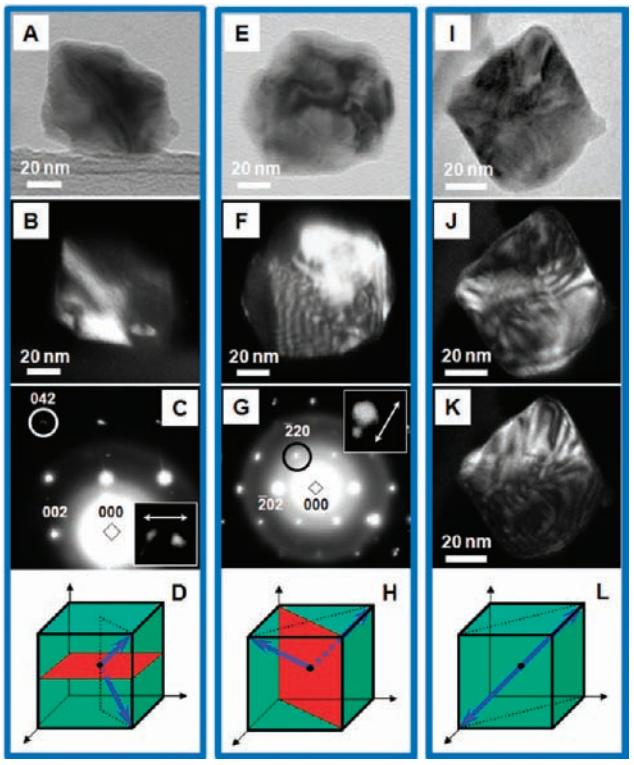

Figure 3. Polarization domains in 100 nm GeTe nanocrystals. (A−C) Bright-field TEM image (A), dark-field TEM image taken with $\vec{g}$ = 002 (B), and corresponding electron diffraction pattern (C) consistent with a (100) twin boundary (109° domain wall). (E−G) Bright-field TEM image (E), dark-field TEM image taken with $\vec{g}$ = $\bar{4}22$ (F), and corresponding electron diffraction pattern (G) consistent with a (110) twin boundary (71° domain wall). (I−K) Bright-field TEM image (I) and dark-field TEM images taken with $\vec{g}$ = 002 (J) and $\vec{g}$ =00$\bar{2}$ (K), respectively, indicating reversal of domain contrast characteristic of an inversion domain boundary (180° domain wall). (D,H,L) Schematic illustrations of the relationships between polarization vectors across 109°, 71°, and 180° domain walls.

particles, resulting in the formation of highly faceted nanostructures of regular diameter exhibiting surface features with a length scale of approximately 30 nm (Figure 4). Electron diffraction patterns of these crystals reveal similar splitting of diffraction spots, indicative of {100} and {110} twin boundary formation (Figure 4C,D, and SI, Figure S5), and exhibit no evidence of diffraction rings characteristic of polycrystals. Dark-field TEM imaging (SI, Figure S6) shows a complex contrast pattern with many strongly diffracting regions, suggesting the presence of numerous polarization domains in the particles. This is consistent with the observed splitting of diffraction spots along multiple directions (Figures S5 and S6), indicating a polydomain state. Sequential addition of precursor to these structures thus results in the formation of networks of polarization domains rather than simple conformal addition of material to the particle surface. These observations suggest an average domain size of approximately 20−50 nm, consistent with literature reports on GeTe thin films.[22]

The formation of domain boundaries in polar-ordered materials arises from a balance among electrostatic energy, elastic energy, and the energy of domain wall formation.[23] Periodic arrays of ferroelastic domain walls form to alleviate epitaxial strains in thin films[24] or strains imposed by surrounding grains in

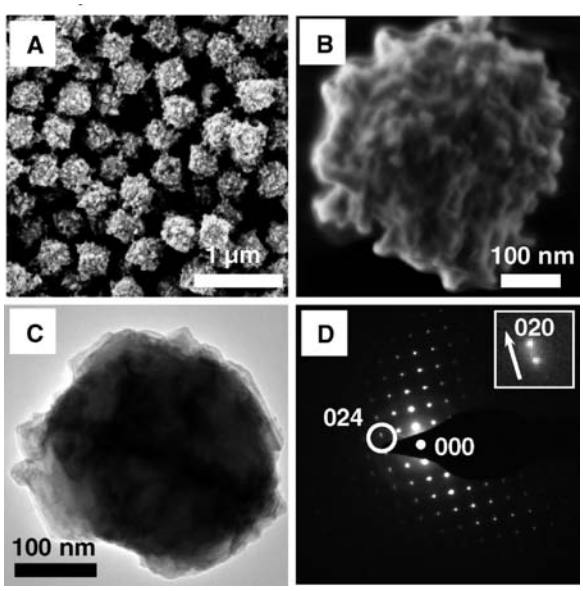

Figure 4. Polarization domains in highly faceted GeTe nanostructures. (A,B) Scanning electron microscope images of highly faceted GeTe nanostructures. (C) TEM image and (D) corresponding electron diffraction pattern of a single GeTe nanostructure illustrating splitting of diffraction spots consistent with {100} twin boundary formation. Inset: Splitting of the 024 diffraction spot along the 020 direction.

ceramic materials.[25] Ferroelastic domain formation is disfavored, however, in unconstrained crystals[26] but has nonetheless been observed in free-standing $BaTiO_3$ films due to the intrinsic tension imposed by a surface layer with different structural properties.[26] Domain formation in our GeTe nanocrystals may proceed via a similar mechanism. Although the high carrier density in GeTe may significantly screen the polarization, an additional electrostatic driving force for domain walls may be present. The formation of purely ferroelectric 180° walls[23] suggests an electrostatic influence on domain formation.

This study demonstrates the synthesis of nanocrystals of the semiconductor GeTe with controlled sizes and narrow size distributions using colloidal techniques. Preliminary analysis indicates the presence of a rhombohedral distortion and polarization domains with a characteristic size scale of ∼30−50 nm. Detailed studies to elucidate the size-dependent polar ordering in these materials are currently underway. These particles should serve as a basis for future fundamental studies of ferroelectric ordering and phase transitions at reduced dimensions and the complex interrelationships between structural, electronic, optical, and other parameters in IV−VI materials.

■ ASSOCIATED CONTENT

Supporting Information. Materials and methods for all syntheses and experiments, TEM images of Ge nanocrystals, additional SEM images, TEM images, electron diffraction patterns, and diffraction results for GeTe nanomaterials. This material is available free of charge via the Internet at http://pubs.acs.org.

■ AUTHOR INFORMATION

Corresponding Author
rramesh@berkeley.edu; alivis@berkeley.edu

■ ACKNOWLEDGMENT

The authors thank Dmitri Talapin, Jonathan Owen, Ronald Gronsky, Jeffrey Urban, and Delia Milliron for helpful discussions and Paul Trudeau for technical assistance. Transmission electron microscopy work performed at the National Center for Electron Microscopy, Lawrence Berkeley National Laboratory, was supported by the Office of Science, Office of Basic Energy Sciences, of the U.S. Department of Energy under Contract No. DE-AC02-05CH11231. The remainder of this work was supported under the Physical Chemistry of Nanocrystals Project of the Director, Office of Science, Office of Basic Energy Sciences, Materials Sciences and Engineering Division, of the U.S. Department of Energy under Contract No. DE-AC02-05CH11231. M.J.P. was supported by a National Science Foundation Graduate Research Fellowship and by a National Science Foundation Integrated Graduate Education and Research Traineeship (IGERT) fellowship.

■ REFERENCES

(1) Baumgardner, W. J.; Choi, J. J.; Lim, Y.-F.; Hanrath, T. *J. Am. Chem. Soc.* **2010**, *132*, 9519.
(2) Hickey, S. G.; Waurisch, C.; Rellinghaus, B.; Eychmueller, A. *J. Am. Chem. Soc.* **2008**, *130*, 14978.
(3) Kovalenko, M. V.; Heiss, W.; Shevchenko, E. V.; Lee, J.-S.; Schwinghammer, H.; Alivisatos, A. P.; Talapin, D. V. *J. Am. Chem. Soc.* **2007**, *129*, 11354.
(4) Littlewood, P. B. *J. Phys. C: Solid State Phys.* **1980**, *13*, 4855.
(5) Waghmare, U. V.; Spaldin, N. A.; Kandpal, H. C.; Seshadri, R. *Phys. Rev. B* **2003**, *67*, 125111.
(6) Andrikopoulos, K. S.; Yannopoulos, S. N.; Voyiatzis, G. A.; Kolobov, A. V.; Ribes, M.; Tominaga, J. *J. Phys.: Condens. Matter* **2006**, *18*, 965.
(7) Lencer, D.; Salinga, M.; Grabowski, B.; Hickel, T.; Neugebauer, J.; Wuttig, M. *Nat. Mater.* **2008**, *7*, 972.
(8) Steigmeier, E. F.; Harbeke, G. *Solid State Commun.* **1970**, *8*, 1275.
(9) Goldak, J.; Barrett, C. S.; Innes, D.; Youdelis, W. *J. Chem. Phys.* **1966**, *44*, 3323.
(10) Chattopadhyay, T.; Boucherle, J. X.; Von Schnering, H. G. *J. Phys. C: Solid State Phys.* **1987**, *20*, 1431.
(11) Snykers, M.; Delavignette, P.; Amelinckx, S. *Mater. Res. Bull.* **1972**, *7*, 831.
(12) Tuan, H.-Y.; Korgel, B. A. *Cryst. Growth Des.* **2008**, *8*, 2555.
(13) Meister, S.; Peng, H.; McIlwrath, K.; Jarausch, K.; Zhang, X. F.; Cui, Y. *Nano Lett.* **2006**, *6*, 1514.
(14) Yu, D.; Wu, J.; Gu, Q.; Park, H. *J. Am. Chem. Soc.* **2006**, *128*, 8148.
(15) Buck, M. R.; Sines, I. T.; Schaak, R. E. *Chem. Mater.* **2010**, *22*, 3236.
(16) Caldwell, M. A.; Raoux, S.; Wang, R. Y.; Philip Wong, H.-S.; Milliron, D. J. *J. Mater. Chem.* **2010**, *20*, 1285.
(17) Urban, J. J.; Yun, W. S.; Gu, Q.; Park, H. *J. Am. Chem. Soc.* **2002**, *124*, 1186.
(18) Adireddy, S.; Lin, C.; Cao, B.; Zhou, W.; Caruntu, G. *Chem. Mater.* **2010**, *22*, 1946.
(19) O'Brien, S.; Brus, L.; Murray, C. B. *J. Am. Chem. Soc.* **2001**, *123*, 12085.
(20) Enders, P. *Phys. Stat. Sol. B* **1983**, *120*, 735.
(21) Snykers, M.; Serneels, R.; Delavignette, P.; Gevers, R.; Van Landuyt, J.; Amelinckx, S. *Phys. Stat. Sol. A* **1977**, *41*, 51.
(22) Yashina, L. V.; Puettner, R.; Neudachina, V. S.; Zyubina, T. S.; Shtanov, V. I.; Poygin, M. V. *J. Appl. Phys.* **2008**, *103*, 094909.
(23) Lines, M. E.; Glass, A. M. *Principles and Applications of Ferroelectrics and Related Materials*; Clarendon Press: Oxford, 1977; pp 87−102.
(24) Roitburd, A. L. *Phys. Stat. Sol. A* **1976**, *37*, 329.
(25) Arlt, G. *J. Mater. Sci.* **1990**, *25*, 2655.
(26) Luk'yanchuk, I. A.; Schilling, A.; Gregg, J. M.; Catalan, G.; Scott, J. F. *Phys. Rev. B* **2009**, *79*, 144111.